Differential roles of PtdIns(4,5)P2 and phosphorylation in moesin activation during Drosophila development.

Fernando Roch, Cédric Polesello, Chantal Roubinet, Marianne Martin, Christian Roy, Philippe Valenti, Sébastien Carreno, Paul Mangeat, François Payre

Differential roles of PtdIns(4,5)P_2 and phosphorylation in moesin activation during *Drosophila* development

Fernando Roch[1,2,*], Cédric Polesello[1,2], Chantal Roubinet[1,3,2], Marianne Martin[4], Christian Roy[4], Philippe Valenti[1,2], Sébastien Carreno[3], Paul Mangeat[4,5] and François Payre[1,2,*]

[1]Université de Toulouse UPS, Centre de Biologie du Développement, Bâtiment 4R3, 118 route de Narbonne, Toulouse, 31062, France
[2]CNRS, UMR5547, Centre de Biologie du Développement, Toulouse, F-31062, France
[3]Institute for Research in Immunology and Cancer, Department of Pathology and Cell Biology, Faculty of Medicine, Université de Montréal, 2900 Édouard-Montpetit Boulevard, Marcelle-Coutu Pavilion Quai 20, Montreal, QC H3T 1J4, Canada
[4]Université de Montpellier II and CNRS, Laboratoire de Dynamique Moléculaire des Interactions Membranaires, Place E. Bataillon, Montpellier, 34095 Cedex 05, France
[5]Université de Montpellier II and CNRS, CRBM, 1919 Route de Mende, Montpellier, 34293 Cedex 05, France
*Authors for correspondence (roch@cict.fr; payre@cict.fr)

Accepted 25 March 2010
Journal of Cell Science 123, 2058-2067

doi:10.1242/jcs.064550

Summary

The ezrin, radixin and moesin (ERM) proteins regulate cell membrane architecture in several cellular contexts. Current models propose that ERM activation requires a PtdIns(4,5)P_2-induced conformational change, followed by phosphorylation of a conserved threonine. However, how these inputs contribute in vivo to orchestrate ERM activation is poorly understood. We addressed this issue by evaluating the contribution of PtdIns(4,5)P_2 and phosphorylation to the regulation of moesin during *Drosophila* development. Unexpectedly, we found that a form of moesin that cannot be phosphorylated displayed significant activity and could substitute for the endogenous product during wing morphogenesis. By contrast, we also show that PtdIns(4,5)P_2 binding is essential for moesin recruitment to the membrane and for its subsequent phosphorylation. Our data indicate that PtdIns(4,5)P_2 acts as a dosing mechanism that locally regulates ERM membrane recruitment and activation, whereas cycles of phosphorylation and dephosphorylation further control their activity once they have reached the cell cortex.

Key words: ERM proteins, Actin cytoskeleton, PtdIns(4,5)P_2, Moesin, *Drosophila* morphogenesis

Introduction

In eukaryotic cells, the organisation and dynamic properties of the plasma membrane depend on a finely regulated interplay between the lipid bilayer and the subjacent cortical actin cytoskeleton, which work together as a single functional unit. Proteins of the ezrin, radixin and moesin (ERM) family act as dynamic linkers between the actin cytoskeleton and the plasma membrane and hence are implicated in the regulation of membrane organisation in numerous cellular and developmental processes (Bretscher et al., 2002; Polesello and Payre, 2004). ERM proteins cycle between an active form, which interacts with both membrane proteins and actin filaments, and a dormant form that localises in the cytoplasm. The dormant conformation is stabilised by an intramolecular interaction that occurs between the N-terminal region (FERM domain) and the C-terminal tail, which contains the F-actin-binding domain (Gary and Bretscher, 1995; Turunen et al., 1994). Adoption of an open, active conformation requires disruption of this interaction in ERM proteins, which unmasks the F-actin-binding region and frees the FERM domain for interaction with its membrane partners.

Two regulatory mechanisms are known to participate in ERM protein activation. First, structural data show that phosphorylation of a conserved threonine residue in the C-terminal domain hinders the intramolecular interaction between FERM and the C-terminus, favouring the open conformation (Matsui et al., 1998; Pearson et al., 2000). Accordingly, many studies suggest that phosphorylation is a key factor controlling ERM activity in vivo (Carreno et al., 2008; Chorna-Ornan et al., 2005; Hayashi et al., 1999; Hipfner et al., 2004; Polesello et al., 2002). Second, evidence obtained from biochemical and cellular assays shows that ERM proteins directly bind to phosphatidylinositol-(4,5)bisphosphate [PtdIns(4,5)P_2], which also promotes their activation (Barret et al., 2000; Nakamura et al., 1999; Niggli et al., 1995; Yonemura et al., 2002). Indeed, studies focusing on the mammalian ezrin have shown that PtdIns(4,5)P_2 binding is a prerequisite for its subsequent phosphorylation (Fievet et al., 2004). Thus, PtdIns(4,5)P_2 is generally envisaged as a membrane cofactor, with specific kinases or phosphatases being the chief players controlling the dynamic aspects of ERM protein regulation. However, recent reports in some cellular contexts show that drastic fluctuations of PtdIns(4,5)P_2 levels have a rapid impact on ERM activation, indicating that the level of PtdIns(4,5)P_2 could have an instructive role on ERM protein activity (Hao et al., 2009; Rasmussen et al., 2008).

To bring new insight into the in vivo mechanisms activating ERM proteins, we evaluated the respective contributions of PtdIns(4,5)P_2 and phosphorylation to the dynamic regulation of ERM proteins during morphogenesis. For this, we developed a genetic approach, focusing on the influence of these two regulatory inputs on the activity of the sole *Drosophila* ERM representative, the moesin protein (Moe) (McCartney and Fehon, 1996; Polesello et al., 2002). We assessed the localisation and biological activity of engineered Moe variants specifically perturbing these two regulatory events, showing that PtdIns(4,5)P_2 binding targets the Moe protein to specific membrane domains in a phosphorylation-independent process. In fact, as long as it interacts with PtdIns(4,5)P_2, a Moe form that cannot be phosphorylated at T559 displays a substantial degree of activity, which varies depending on the cellular context examined.

In addition, PtdIns(4,5)P_2-dependent membrane recruitment of Moe appears both a prerequisite and the rate-limiting step for its subsequent phosphorylation. By contrast, expression of a Moe phosphomimetic form provokes profound deleterious effects on development, which are only partially suppressed when PtdIns(4,5)P_2 interaction is prevented. Altogether, our data indicate that phosphoinositide levels have an intrinsic role during ERM activation in vivo, with dynamic phosphorylation further contributing to the fine-tuning of ERM activity in specific morphogenetic contexts.

Results

Binding to PtdIns(4,5)P_2 is required for Moe membrane localisation in *Drosophila*

Biochemical studies have shown that human ezrin binds to PtdIns(4,5)P_2 (Barret et al., 2000; Niggli et al., 1995). To determine whether this feature also applies to Moe, we analysed its ability to cosediment with liposomes containing increasing concentrations of PtdIns(4,5)P_2 under conditions of physiological ionic strength (Niggli et al., 1995). We observed a clear positive correlation between the amount of PtdIns(4,5)P_2 present in the liposomes and the proportion of Moe associated with these vesicles (Fig. 1A). Conversely, Moe did not associate with liposomes containing only phosphatidylcholine or supplemented with either phosphatidylserine or phosphatidylethanolamine, indicating that Moe interacts with PtdIns(4,5)P_2 and not with other common membrane phospholipids (Fig. 1B). Similarly to ezrin (Barret et al., 2000), substitution in the Moe protein of two conserved lysine doublets (K254-K255 and K263-K264) by asparagines (MoeKN form) abolished binding to PtdIns(4,5)P_2 (Fig. 1C), whereas its weak affinity for other phospholipids was not altered (Fig. 1A,B). Thus, although we cannot rule out an interaction of Moe with other phosphoinositides, these results indicate that this ERM protein, like ezrin, binds to PtdIns(4,5)P_2.

To evaluate the influence of PtdIns(4,5)P_2 binding on the subcellular distribution of Moe, we expressed different mutant GFP-tagged versions of these proteins in *Drosophila* S2 cells. The MoeWT-GFP protein was seen in the cytoplasm and also associated with F-actin-rich structures in the cell cortex (Fig. 2A). By contrast, MoeKN-GFP did not accumulate in the membrane and localised preferentially in the cytoplasm (Fig. 2B,G). Although significant amounts of a Moe form that cannot be phosphorylated (MoeTA-GFP, carrying the T559A mutation) were still seen associated with the cortex (Fig. 2C,G), the double mutant MoeKNTA-GFP behaved in a similar manner to MoeKN-

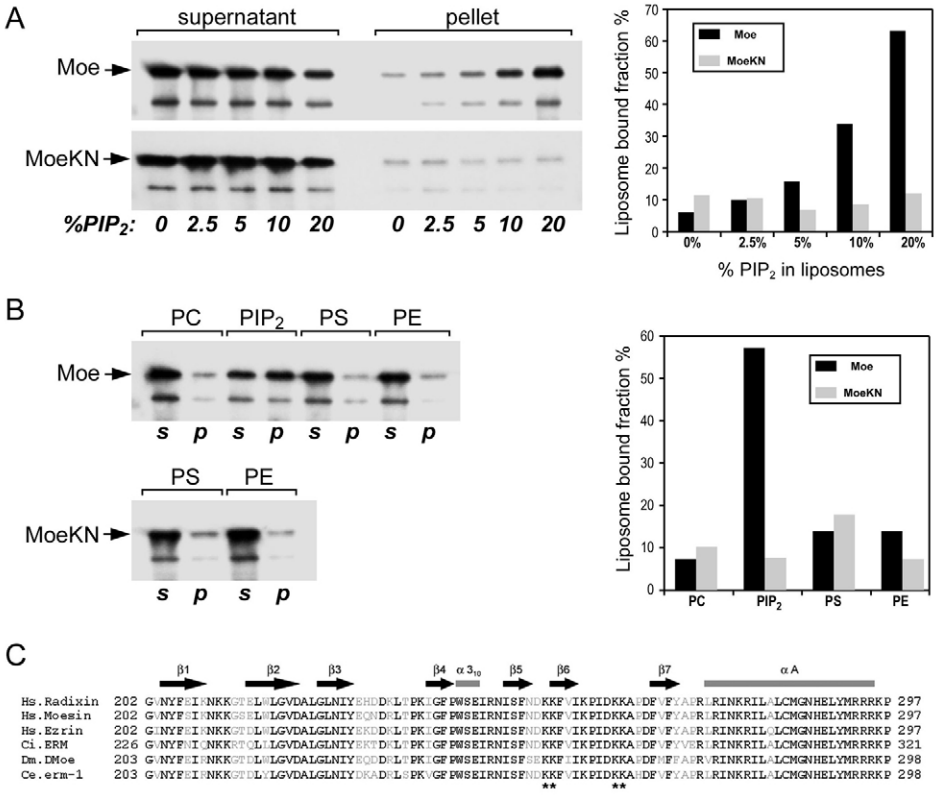

Fig. 1. *Drosophila* Moe binds to PtdIns(4,5)P_2 in a liposome co-sedimentation assay. (**A**) MoeWT and MoeKN association with phosphatidylcholine liposomes containing increasing concentrations of PtdIns(4,5)P_2. The supernatant contains the free Moe fraction, whereas the pellet contains the lipid-associated Moe. Full-length Moe (upper panel, arrow) but not full-length MoeKN (lower panel, arrow) binds to PtdIns(4,5)P_2-containing liposomes. The graph shows the percentage of Moe protein recovered in each fraction. (**B**) Full-length wild-type Moe (upper panel, arrow) and full-length MoeKN (lower panel, arrow) found in the supernatant (s) or pellet (p) fractions, after incubation with liposomes containing either 100% phosphatidylcholine (PC) or supplemented with 20% PtdIns(4,5)P_2 (PIP$_2$), 20% phosphatidylserine (PS) or 20% phosphatidylethanolamine (PE). The graph illustrates the percentage of Moe protein found associated with liposomes in each condition. Wild-type Moe associates with liposomes in the presence of PtdIns(4,5)P_2, but not other phospholipids, whereas MoeKN is never found associated with liposomes. (**C**) Sequence alignment corresponding to the F3 FERM subdomain of six different ERM proteins (human: NP_002879, NP_002435 and NP_003370; *Ciona*: NP_001027599; *Drosophila*: P46150; and *Caenorhabditis*: NP_491559). Invariant amino acids are highlighted in black. The two Lys doublets substituted by Asn are indicated with asterisks. Above the alignment is shown the secondary structure of the F3 subdomain (β-strand, black arrow; α-helix, grey box). The Lys doublets are in the cytosol-exposed loops of the FERM domain (Pearson et al., 2000).

GFP and was cytoplasmic (Fig. 2D,G). As previously observed (Kunda et al., 2008), the phosphomimetic form MoeTD-GFP (T559D) appeared enriched in the cortex and its expression induced formation of ectopic F-actin structures at the membrane (Fig. 2E,G). In addition, MoeTD-GFP elicited clear morphological defects: cells appeared contracted and rounded (Fig. 2E,H). However, when combined with KN mutations, the phosphomimetic version MoeKNTD-GFP localised at the cortical level, similarly to MoeWT-GFP (Fig. 2F,G). Therefore, the presence of the phosphomimetic mutation promotes Moe access to the cell cortex, even when PtdIns(4,5)P_2 binding is impaired. However, MoeKNTD-GFP expression did not induce morphological alterations, unlike MoeTD-GFP (Fig. 2F,H).

Regulation of Moe activity by PtdIns(4,5)P_2 is crucial for fly morphogenesis

To test the activity of these different Moe variants in vivo, we monitored their ability to substitute for the endogenous product during fly development. We generated transgenic lines expressing Moe mutant forms under the control of an UAS promoter (Brand and Perrimon, 1993) and selected those that, upon induction with the ubiquitous *tubulin-GAL4*^{LL7} driver, produced Moe levels comparable with those seen for the endogenous protein (supplementary material Fig. S1A). We then analysed whether the different Moe versions could rescue the phenotypes associated with the two loss of function alleles *Moe*^{PL106} and *Moe*^{PL54}, both caused by P-element insertions in different *Moe* regulatory regions (Polesello et al., 2002). The *Moe*^{PL106} mutant allele leads to lethality during late development, but we observed *Moe*^{PL106} adult escapers appearing at low frequency in our fly cultures. Wings of these escapers were often crumpled and reduced in size and their eyes displayed a rough-eye phenotype, because ommatidia were reduced in number and appeared disorganised (Fig. 3A). We also tested the rescuing properties of Moe variants using *Moe*^{PL54}, the strongest available *Moe* allele, which leads to 100% lethality in embryonic or early larval stages.

Expression of MoeWT-GFP greatly enhanced the viability and restored the visible phenotypes of both *Moe*^{PL106} and *Moe*^{PL54} mutants (Fig. 3A,B). However, MoeKNTA-GFP showed little rescuing activity, confirming that PtdIns(4,5)P_2 binding and T559 phosphorylation are the major events controlling Moe activation in vivo. In contrast to previous reports (Hipfner et al., 2004; Speck et al., 2003), we found that expression of MoeTD-GFP did not rescue the mutant phenotypes and instead provoked lethality in both *Moe* mutants and wild-type siblings. Thus, MoeTD-GFP interferes with normal development, mirroring the deleterious effects observed in S2 cells. Unexpectedly, we also observed that all lines expressing MoeTA-GFP significantly enhanced the viability of *Moe*^{PL106} flies. In addition, the wings of these rescued animals showed wild-type morphology, indicating that MoeTA-GFP retains some activity (Fig. 3A). However, *Moe*^{PL106} mutants rescued by MoeTA-GFP still exhibited obvious eye phenotypes, confirming that Moe phosphorylation is essential for proper morphogenesis in this tissue (Fig. 3A). By contrast, MoeKN-GFP, which cannot bind to PtdIns(4,5)P_2, retained only a weak activity, because it slightly enhanced *Moe*^{PL106} viability. In addition, these escapers had rough eyes and crumpled wings, suggesting that Moe PtdIns(4,5)P_2-binding activity is necessary for the morphogenesis of these tissues (Fig. 3A,B). Finally, we observed that the toxic effects induced by expression of MoeTD-GFP were suppressed if its interaction with PtdIns(4,5)P_2 was prevented. Indeed, expression of MoeKNTD-

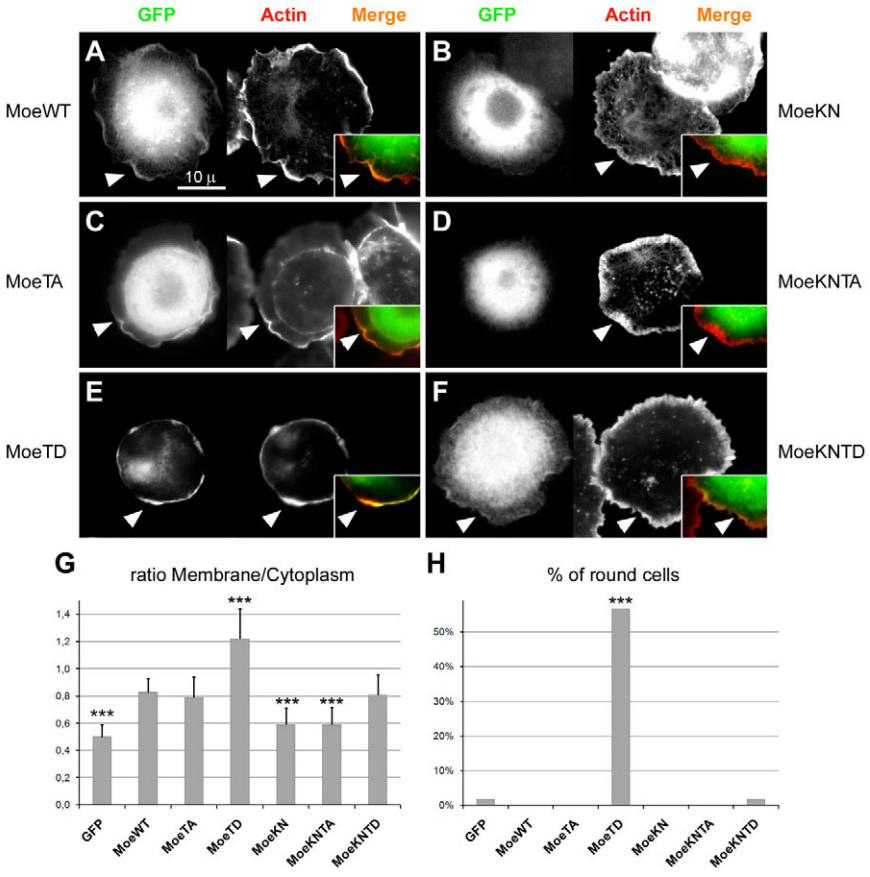

Fig. 2. PtdIns(4,5)P_2 binding is required for Moe localisation in *Drosophila* S2 cells. S2 cells transfected to express the different Moe-GFP mutant versions (right panels, green in merge insets) were stained with Rhodamine-phalloidin to reveal F-actin (left panels, red in merge insets). (**A**) In addition to a cytoplasmic distribution, MoeWT-GFP colocalises with F-actin at the cell cortex (arrowheads). Scale bar: 10 µm. (**B**) MoeKN-GFP does not associate with the cortex and remains in the cytoplasm. (**C**) MoeTA-GFP shows colocalisation with F-actin at the cell periphery (arrowheads). (**D**) The MoeKNTA-GFP double mutant localises exclusively in the cytoplasm. (**E**) Cells expressing MoeTD-GFP have an abnormal contracted morphology, displaying a characteristic round shape. We detected increased levels of MoeTD-GFP at the cell cortex, compared with MoeWT-GFP (arrowheads). (**F**) MoeKNTD-GFP does not induce morphological alterations and is found both in the cytoplasm and at the F-actin cortex (arrowheads). (**G**) Graph presenting the membrane/cytoplasm signal ratios observed in cells expressing the different Moe-GFP versions. Free GFP is shown as control. Error bars indicate s.d. (n=20 for each construct). Distributions significantly different from that of MoeWT-GFP are labelled with asterisks (***$P<10^{-4}$ in Student's t-tests). (**H**) Proportion of cells displaying a rounded morphology, estimated as the percentage of cells presenting a circularity index [π*area/sqr(perimeter)]>0.98. A value of 1.0 indicates a perfect circle (n=60 for each construct).

GFP also enhanced the viability of Moe^{PL106} flies and restored the wing phenotypes (Fig. 3A,B). However, MoeKNTD-GFP did not rescue the eye phenotype, and elicited even stronger eye defects in Moe^{PL106} adults (Fig. 3A).

Since our rescuing assays used GFP-tagged proteins, it remained possible that the GFP moiety could influence their activity. We therefore produced transgenic lines driving robust expression of a set of equivalent full-length untagged *Moe* variants (supplementary material Fig. S1B). *Moe* mutant flies rescued after expression of these untagged versions showed phenotypes identical to those observed after expression of the corresponding tagged forms (not shown). However, untagged forms better enhanced the viability of the *Moe* mutants, suggesting that addition of a GFP moiety is slightly detrimental for Moe activity. Indeed, expression of untagged MoeTA and MoeKNTD now also rescued the lethality of the strong Moe^{PL54} allele (Fig. 3B and supplementary material Fig. S2), further indicating that these two forms have significant biological activity. We did not observe dominant phenotypes in wild-type flies after expression with *tubulin-GAL4* of the different Moe variants, except in two cases: MoeTD, which caused lethality in early larva and MoeKNTD, whose expression did not affect viability, but elicited a mild rough-eye phenotype.

In summary, our results indicate that in vivo regulation of Moe does not rely exclusively on control of its phosphorylation state. In fact, the form that cannot be phosphorylated (MoeTA) is the variant that displays the highest activity and is able to rescue the strong Moe^{PL54} mutant. By contrast, inhibition of binding to phospholipids has a deeper impact on Moe activity, which can nevertheless be compensated to a limited extent by a concomitant phosphomimetic mutation.

PtdIns(4,5)P_2 binding, but not phosphorylation, is essential for Moe function in wing cells

Our data indicate that Moe regulation by T559 phosphorylation is essential for eye morphogenesis but could have a less-prominent role during wing development. This unexpected result prompted us to characterise at the cellular level how Moe activity is regulated in the developing wing disc, where Moe has been shown to be required for epithelial integrity (Hipfner et al., 2004; Speck et al., 2003). Consistently, we observed wing cells detached from the main epithelium in Moe^{PL106} adult escapers (Fig. 3A). To study this phenotype in a reproducible system, we generated mosaic wing discs containing clones of homozygous *Moe* mutant cells (Fig. 4A-F). All observed Moe^{PL106} mutant clones contained extruding cells in the most basal part of the epithelium (Fig. 4A,D). Most of these cells had pyknotic nuclei (Fig. 4A,D) and expressed high levels of activated Caspase3 (Fig. 4E,F), indicating that they undergo apoptosis. We tested the ability of the different Moe variants to rescue this phenotype when driven exclusively in the Moe^{PL106} mutant cells. Expression of either MoeWT-GFP or MoeTA-GFP prevented the formation of extruding cells in all observed clones, confirming that regulation of Moe by phosphorylation is dispensable for epithelium integrity (Fig. 4G,I). Conversely, we observed apoptotic extruding cells with all the other Moe variants, including MoeKNTD-GFP (Fig. 4H,J-L), which indicates that this form is also unable to provide full rescue activity in the wing cells; a fact that went unnoticed in our escaper analysis probably because of the regulative properties of the wing disc. In fact, the development of this appendage can compensate for substantial amounts of cell death without showing obvious defects.

Analysis of the distribution of these Moe variants in wing cells was also informative. MoeWT-GFP accumulated in F-actin-rich

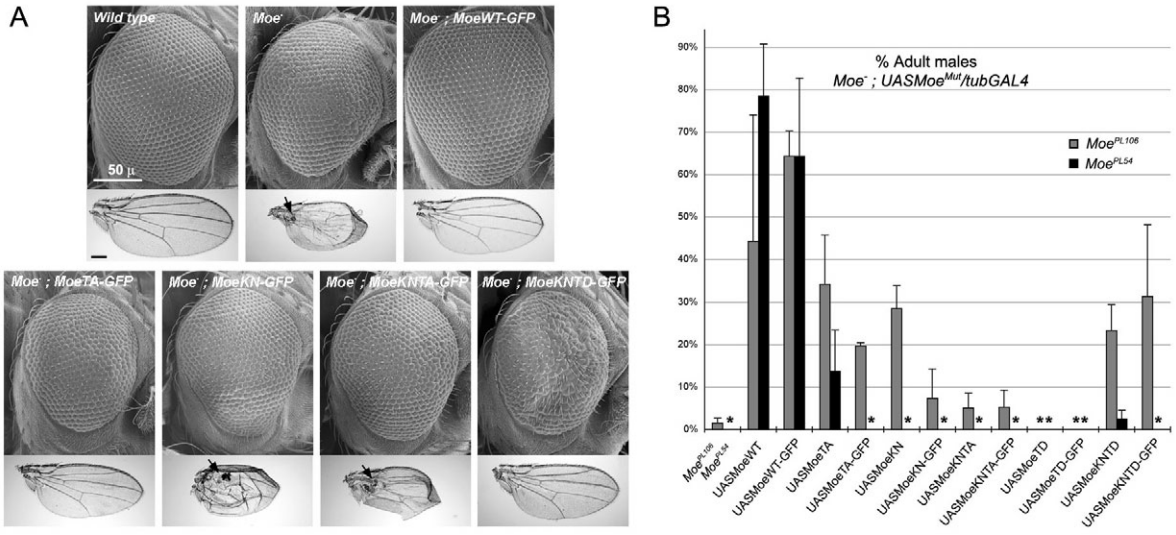

Fig. 3. Testing the biological activity of Moe mutants affecting its phosphorylation and its PtdIns(4,5)P_2 binding ability. (**A**) Scanning electron micrographs of adult eyes and pictures of wings taken from different rescued Moe^{PL106} males. Moe^{PL106} escapers present reduced rough eyes and small crumpled wings displaying cuticle vesicles trapped between the two wing surfaces (black arrows). Expression of MoeWT-GFP completely rescues both wing and eye phenotypes. However, none of the different Moe variants (MoeTA-GFP, MoeKN-GFP, MoeKNTA-GFP and MoeKNTD-GFP) is able to rescue the eye defects. MoeKNTD-GFP-expressing flies show eyes further reduced and more disorganised than the Moe^{PL106} mutants. MoeKN-GFP and MoeKNTA-GFP do not rescue the wing phenotypes, whereas all wings expressing MoeTA-GFP and MoeKNTD-GFP are normal. Scale bars: 50 µm top panels, 250 µm, bottom. (**B**) The histogram represents the percentage of Moe^{PL106} (grey bars) or Moe^{PL54} (black bars) mutant flies reaching the adult stage after rescue with the different Moe versions (males Moe^{-}*; tubulin-GAL4/UASMoe*^{Mut}). Each bar of the histogram corresponds to an average rescue obtained pooling together all the different transgenic lines that code for the same Moe version (see supplementary material Fig. S2). The bars labelled Moe^{PL106} and Moe^{PL54} correspond to the proportion of Moe^{-}*; tubulin-GAL4/+* escapers obtained in control experiments. Asterisks indicate lethal combinations. Error bars correspond to the s.d.

cortical structures and reached its highest levels in the apical-most part of the cell (Fig. 5A). We also detected a weaker and more diffuse signal in the cytoplasm and nucleus (Fig. 4G). The subcellular distribution of MoeTA-GFP was similar, but accumulation in the most apical part of the cells was less prominent (Fig. 5B). By contrast, MoeKN-GFP and MoeKNTA-GFP did not concentrate in F-actin-rich regions and showed diffuse staining, presenting a graded distribution with higher levels in the apical portion of the epithelium (Fig. 4H,J and Fig. 5D,E). MoeTD-GFP was never seen in the cytoplasm and was exclusively found in association with the cell cortex, reaching abnormally high levels in the lateral membrane and triggering ectopic accumulation of F-actin in these regions (Fig. 4K and Fig. 5C). Finally, the MoeKNTD-GFP distribution was more similar to that of MoeWT-GFP and differs from MoeTD-GFP in several aspects: it was readily detected in the cytoplasm, it accumulated preferentially in apical regions and its expression did not affect the organisation of the actin cytoskeleton (Fig. 4L and Fig. 5F).

We have shown that MoeKNTD has some biological activity, because it could improve the viability of *Moe* mutant flies. But can an active phosphorylated form such as MoeKNTD occur in vivo if PtdIns(4,5)P_2-binding is prevented? We tested this possibility using a specific antibody against phosphorylated T559 (Moe-*P*) (Karagiosis and Ready, 2004). As expected, Moe-*P* levels were clearly diminished in Moe^{PL106} mutant clones (Fig. 6A), whereas the Moe-*P* signal was recovered upon reintroduction of MoeWT-GFP in the mutant cells (Fig. 6B). However, no Moe-*P* signal was detected in mutant cells expressing the MoeKN-GFP form (Fig. 6C), a result confirmed in immunoblots of protein extracts obtained from Moe^{PL106} adult flies expressing either MoeKN-GFP or MoeKN (Fig. 6D).

Thus, our results indicate that PtdIns(4,5)P_2 binding has an essential role in the wing epithelium: it is a prerequisite for Moe phosphorylation and is essential to localise Moe to the cell cortex. By contrast, T559 phosphorylation appears to be dispensable in this tissue both for cortical accumulation of Moe and Moe activity.

The distribution of PtdIns(4,5)P_2 affects Moe localisation in the wing epithelium

PtdIns(4,5)P_2 binding seems to be required for in vivo regulation of Moe activity. One possibility is that PtdIns(4,5)P_2 could regulate the subcellular localisation of Moe. To test this hypothesis, we visualised the distribution of PtdIns(4,5)P_2 in wing cells by studying the localisation of a phospholipase C (PLC) δ1 pleckstrin-homology domain coupled to GFP (PH-GFP), a protein probe that binds specifically to PtdIns(4,5)P_2 (Stauffer et al., 1998; Zelhof and Hardy, 2004). In wild-type wing cells, PH-GFP was seen associated with the cortex throughout the cells, accumulating at high levels in the apical domain (Fig. 7A). This distribution was similar to that observed for MoeTA-GFP (Fig. 7E), which is consistent with the idea that in the absence of T559 phosphorylation, PtdIns(4,5)P_2 controls the subcellular localisation of Moe.

To further evaluate this possibility, we increased the cellular levels of PtdIns(4,5)P_2 and monitored the consequences on Moe localisation. Type I phosphatidylinositol kinases (PIP5KIs) have a prominent role in the synthesis of PtdIns(4,5)P_2 from the PtdIns(4)*P* precursor (Yin and Janmey, 2003). In *Drosophila*, the *skittles* (*sktl*) locus codes for a PIP5KI (Hassan et al., 1998). Upon ectopic

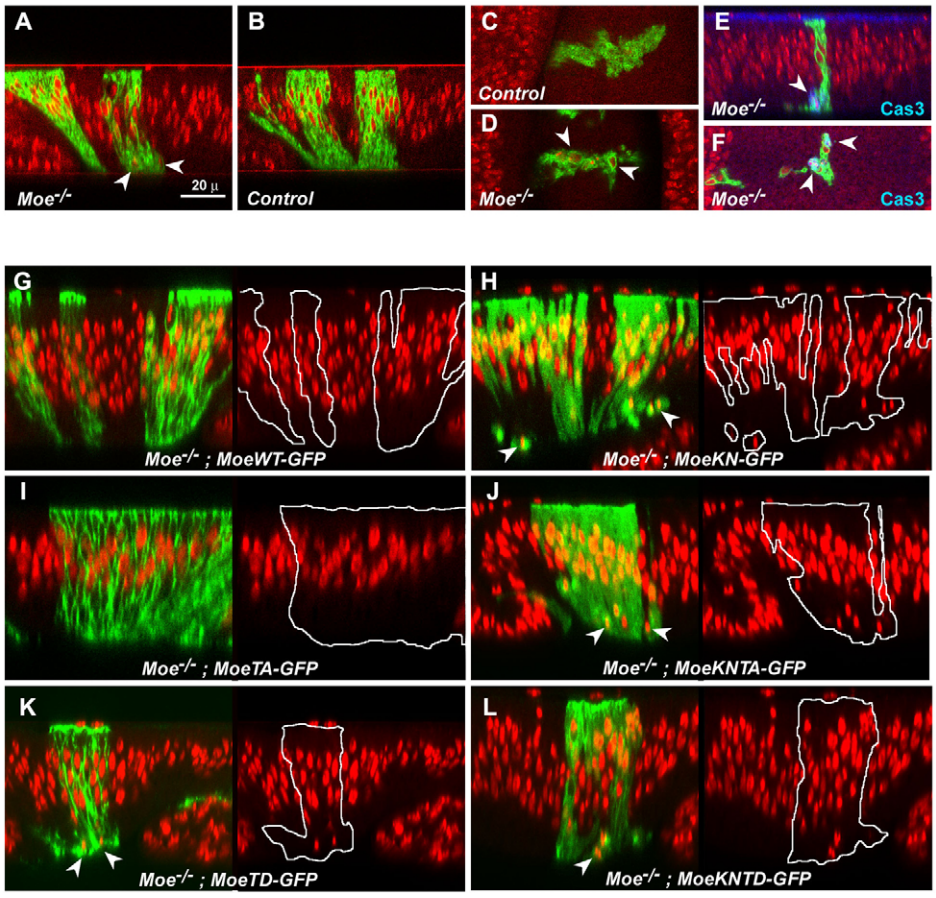

Fig. 4. Functional analysis of Moe regulation in the wing-disc epithelium. All pictures are confocal longitudinal sections of third larval instar wing epithelia (apical is up, basal is down) except panels C, D and F, which correspond to transverse optical sections showing the basal part of the disc. Nuclei are labelled with Topro3 (red), whereas E and F are also stained with an activated Caspase3-specific antibody (blue). All images were taken at the same magnification. Scale bar: 20 µm. (**A-F**) Control or $Moe^{-/-}$ mutant cells are labelled positively with mCD8GFP (green). Pyknotic nuclei corresponding to extruded $Moe^{-/-}$ mutant cells (arrowheads) are found in the basal part of the imaginal disc (compare A,D with controls in B,C). (E-F) Extruded cells are apoptotic and express activated Caspase3 (arrowheads). (**G-L**) Wing discs containing *Moe* mutant clones expressing autonomously the different MoeGFP-tagged versions (GFP distribution is shown in green). The adjacent right panels show the nuclei distribution, with clone position marked by a white contour. Expression of MoeWT-GFP (G) but also of MoeTA-GFP (I) rescues the $Moe^{-/-}$ cell extrusion phenotype, whereas apoptotic cells (arrowheads) are still found in clones expressing MoeTD-GFP (K) or any of the forms not binding to PtdIns(4,5)P_2: MoeKN-GFP (H), MoeKNTA-GFP (J) and MoeKNTD-GFP (L).

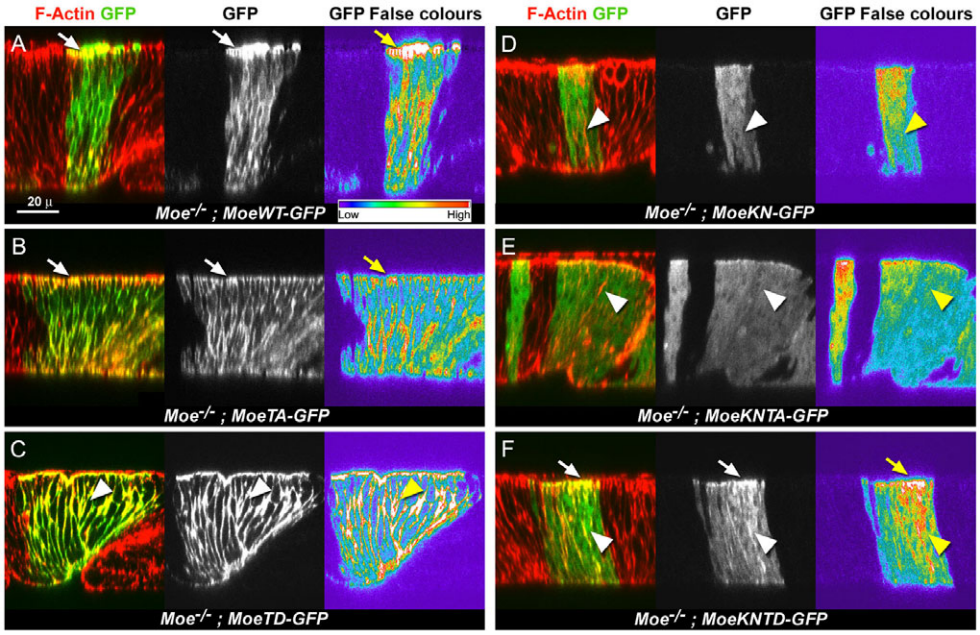

Fig. 5. Subcellular distribution of Moe-GFP mutants in the wing epithelium. Confocal longitudinal sections of third larval instar wing discs stained with Rhodamine-phalloidin to reveal F-actin (red). The discs contain *Moe* mutant clones expressing autonomously the different Moe-GFP tagged variants (GFP distribution shown in green, in greyscale panels and in false colours). Scale bar: 20 µm. (**A**) The MoeWT-GFP protein accumulates at the cell cortex in F-actin rich regions, especially in the apical part (arrows). It is also detected in the cytoplasm. (**B**) MoeTA-GFP is similarly distributed, but its apical accumulation is less prominent (arrows). (**C**) MoeTD-GFP is associated with the cell cortex and is observed at high levels in lateral regions, which accumulate high levels of F-actin (arrowheads). (**D**) MoeKN-GFP does not accumulate in actin-rich regions (arrowhead). (**E**) Similarly, MoeKNTA-GFP is homogenously distributed in the cell body and does not accumulate in the cortex (arrowhead). (**F**) MoeKN-TD is associated with the cortical actin (arrowheads), mostly in the apical region (arrows).

expression of Sktl, PH-GFP accumulated at high levels in the most apical part of the cells (Fig. 7A,B), where we also observed the formation of abnormal membrane protrusions (Fig. 7B,D,F,I,J). This indicates that Sktl overexpression boosts the PtdIns(4,5)P_2 levels in the apical domain of the wing cells, interfering with normal membrane organisation. Raising the PtdIns(4,5)P_2 levels also affected the localisation of both MoeTA-GFP (Fig. 7E,F) and MoeWT-GFP (Fig. 7C,D), which were then over-represented in the apical cortex. By contrast, the distribution of MoeKN-GFP was not altered in the presence of ectopic PtdIns(4,5)P_2 (Fig. 7G,H). We also monitored the phosphorylation state of endogenous Moe in the presence of ectopic Sktl. Our immunostaining revealed abnormal accumulation of Moe-*P* staining in the apical part of Sktl-overexpressing cells (Fig. 7I,J), and we also found increased levels of Moe-*P* in protein extracts obtained from the same discs (Fig. 7K). Thus, our results indicate that high PtdIns(4,5)P_2 levels can recruit Moe to the cell cortex, affecting both its subcellular distribution and its availability as a substrate for phosphorylation.

We also tested whether loss of the *sktl* gene is accompanied by a reduction of the Moe-*P* levels in the wing epithelium. In the ovaries, germ line clones for null *sktl* alleles induce a developmental arrest in early stages, but a clear reduction of Moe-*P* levels was observed in *sktl* hypomorphic backgrounds, which do not hinder ovary early development (Gervais et al., 2008). Wing epithelial integrity is compromised in homozygous mutant cells for the hypomorphic $sktl^{\Delta 5}$ allele (Hassan et al., 1998), because we observed the presence of extruding cells in the most basal part of the disc when apoptosis was prevented by concomitant expression of the p35 anti-apoptotic factor (Hay et al., 1994) (supplementary material Fig. S3A,B). However, we did not detect a significant decrease of the Moe-*P* levels in these mutant cells (supplementary material Fig. S3C-F), a negative result that is difficult to interpret because PtdIns(4,5)P_2 levels could only be slightly reduced in these clones.

Discussion

The aim of this work was to better understand how ERM protein activation is regulated in a developing organism and for this, *Drosophila* morphogenesis constitutes an attractive system in which to analyse the cellular mechanisms involved. We show that two highly conserved mechanisms control Moe activation: PtdIns(4,5)P_2 binding and phosphorylation of the invariant T559 residue. Thus, the study of the regulation of Moe in flies offers conclusions that could be extrapolated to ERM proteins of other species, including mammals. We show that substituting the endogenous Moe by point mutations affecting T559 phosphorylation or PtdIns(4,5)P_2 binding leads to distinguishable morphogenetic defects, thereby allowing genetic dissection of their respective contributions. Our results indicate that the role of PtdIns(4,5)P_2 is not restricted to a pre-activation step and instead, intrinsically regulates Moe subcellular localisation and activity.

Cellular levels of PtdIns(4,5)P_2 control ERM access to the membrane

Previous studies in mammalian cells have shown that ezrin directly binds to PtdIns(4,5)P_2, allowing identification of two lysine doublets in the N-terminal FERM domain that are required for this interaction (Barret et al., 2000). These residues are conserved in the Moe protein and their replacement by asparagines (MoeKN) similarly blocks interaction with PtdIns(4,5)P_2, suggesting that PtdIns(4,5)P_2-binding is an ancient feature shared by all extant ERM proteins.

Our data support the view that these lysine residues act as a PtdIns(4,5)P_2 sensor, permitting efficient membrane recruitment of

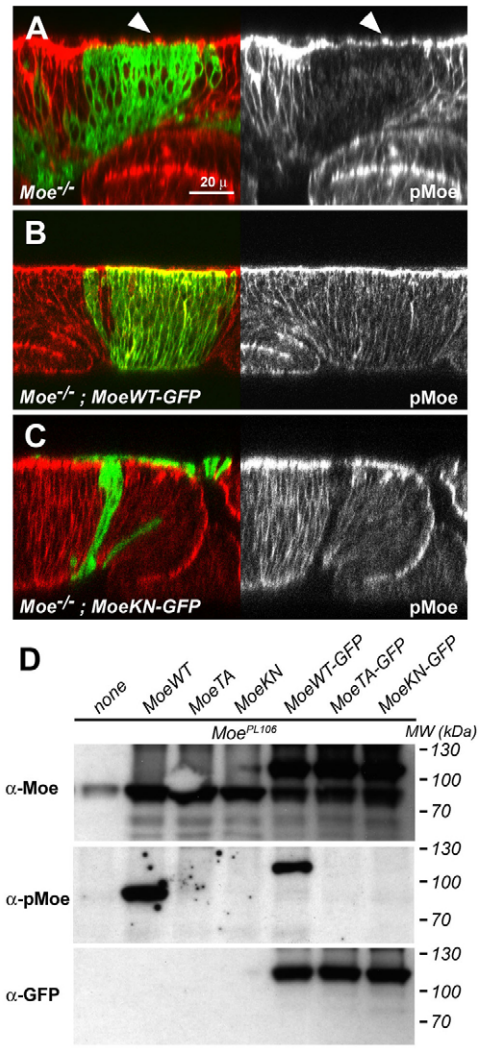

Fig. 6. PtdIns(4,5)P_2 binding is required for in vivo phosphorylation of Moe. (**A-C**) Confocal sections of third larval instar wing discs stained with anti-Moe-*P* (red). Only the red channel is shown on the right (black and white images). (A) *Moe* mutant cells marked by mCD8-GFP (green) show little Moe-*P* staining, except for some unspecific signal found in the nucleus. The staining observed in the most apical part of the disc corresponds to peripodial membrane cells that cover the wing epithelium and show normal accumulation of Moe-*P* (arrowheads). (B) MoeWT-GFP (green) becomes phosphorylated normally when is introduced in the *Moe* cells. (C) No Moe-*P* signal above background levels is detected in *Moe* clones expressing MoeKN-GFP (green). Scale bar: 20 µm. (**D**) Blots showing the relative amounts of total Moe and phosphorylated Moe (pMoe) present in protein extracts of Moe^{PL106} adult males expressing different variants of Moe. Only the MoeWT and MoeWT-GFP proteins are significantly phosphorylated.

ERM proteins from a cytosolic pool of dormant molecules (Fig. 8). In the polarised wing cells, PtdIns(4,5)P_2 is found in the plasma membrane and accumulates in their most apical part – a region containing high levels of Moe. We show that the KN mutations block Moe recruitment to the cell cortex. Conversely, experimental elevation of the PtdIns(4,5)P_2 levels in the apical portion of the cell is accompanied by accumulation in the same region of MoeTA-GFP and MoeWT-GFP, but not MoeKN-GFP. Thus, these observations suggest that PtdIns(4,5)P_2 availability controls Moe access to the cell cortex and has an instructive role during this recruitment step, which can be achieved independently of Moe phosphorylation. Our results confirm that, as with mammalian ezrin (Fievet et al., 2004), Moe phosphorylation cannot be achieved in wing cells if its interaction with PtdIns(4,5)P_2 is hindered by the KN mutations. Thus, PtdIns(4,5)P_2 binding appears to be a prerequisite for subsequent Moe phosphorylation. Moreover, we also observed increased amounts of phosphorylated Moe as a consequence of raising the PtdIns(4,5)P_2 levels in the wing, suggesting that kinase availability is not the limiting factor determining the degree of Moe phosphorylation in this tissue. Previous observations made in the fly ovary reported a reduction of phosphorylated Moe levels in mutant clones for a PIP5K *sktl* hypomorphic allele (Gervais et al., 2008). However, we did not observe the same reduction in the wing cells. This discrepancy might reflect the existence of genuine tissue differences affecting Moe regulation, but it is difficult to draw a conclusion at this stage, owing to possible genetic redundancy with other PIP5Ks encoded by *Drosophila* (for instance, the *PIP5K59B* gene) and the specific nature of the available *sktl* hypomorphic alleles, which all affect regulatory sequences that could be tissue specific (Gervais et al., 2008; Hassan et al., 1998).

Our genetic assays revealed that MoeKN still retains a low biological activity. If the KN mutations prevent PtdIns(4,5)P_2 binding, how can this protein still link F-actin to the cell cortex? Interestingly, recent work has shown that membrane association of vertebrate moesinKNTD and ezrinKNTD is sensitive to PtdIns(4,5)P_2 (Hao et al., 2009). Thus, although mutation of the lysine doublets prevents efficient access to the membrane, it does not completely abolish interaction with PtdIns(4,5)P_2, which contributes to maintain ERM KNTD forms in the cortex. Crystallographic analyses of InsP_3-complexed Radixin show that the presumptive PtdIns(4,5)P_2-interacting region is a cleft that is present in a highly positively charged surface of the FERM domain (Hamada et al., 2000). Interestingly, the two conserved lysine doublets are in this charged surface, but not located in the cleft that interacts with InsP_3. It is tempting to speculate that PtdIns(4,5)P_2 could first interact with the charged surface of ERM proteins and favour membrane recruitment before lodging into the cleft and promote ERM activation. Our results suggest that a small fraction of MoeKN could reach the membrane compartment, presumably by stochastic motion, and then interact with PtdIns(4,5)P_2 via its intact FERM cleft. The fly MoeKNTD form is more efficiently recruited to the cortex and displays a higher activity than MoeKN because this open molecule can also interact with F-actin. Indeed, MoeKNTD is found preferentially in regions rich in F-actin. Finally, MoeTD displays the highest affinity for the cortex because of its ability to bind both PtdIns(4,5)P_2 and F-actin. Moreover, its presence in the cortex triggers accumulation of F-actin, which in turn could allow further recruitment of MoeTD, as seen in both S2 cells and lateral regions of wing cells.

Moe phosphorylation in T559 is not essential for its activation

A surprising finding of our studies is that a Moe form that cannot be phosphorylated in T559 still displays significant activity in various developmental processes. Although overexpression of such forms partly counteracts endogenous ERM protein activity in both wild-type and pathological contexts (Carreno et al., 2008; Chorna-Ornan et al., 2005; Khanna et al., 2004; Polesello et al., 2002; Yu et al., 2004), our genetic assays show that MoeTA has a rescuing activity in the absence of the endogenous product. MoeTA, which can associate with the membrane, significantly improves the

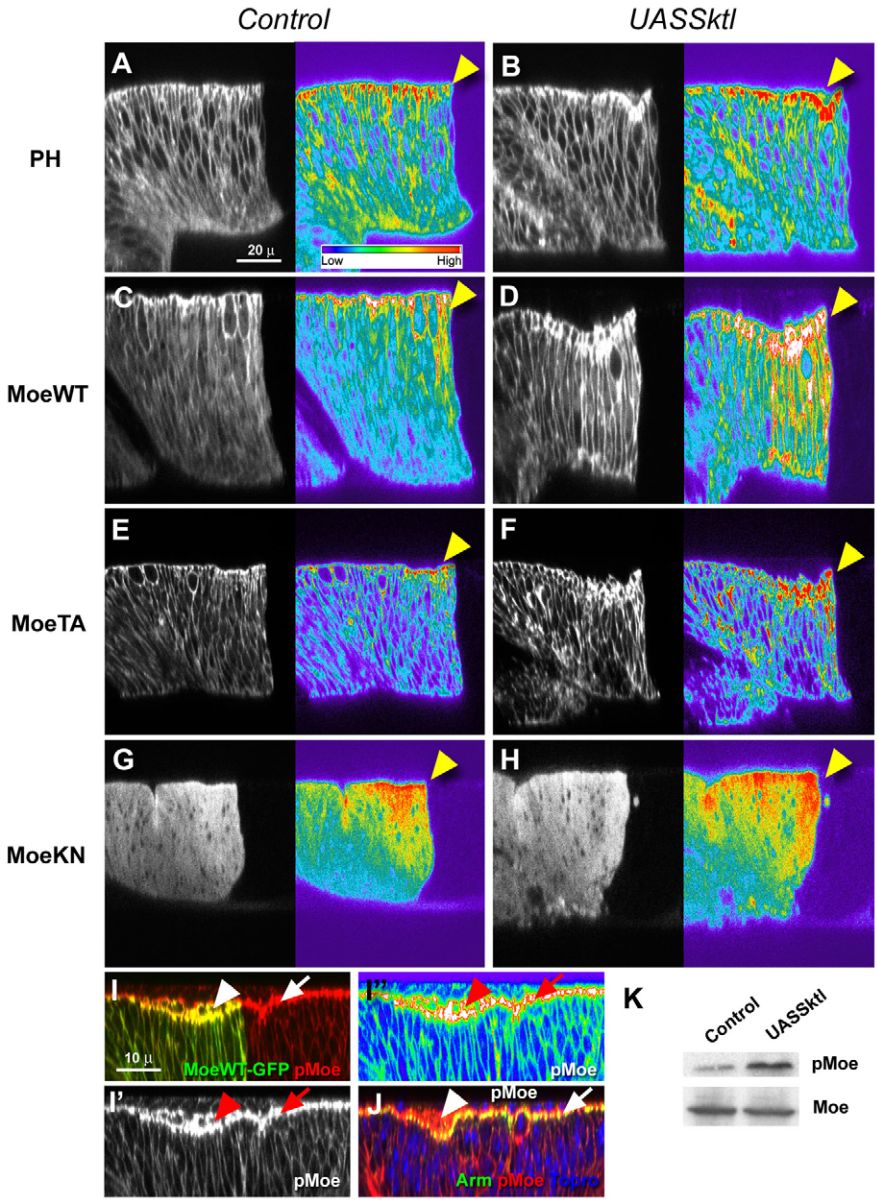

Fig. 7. Increasing levels of PtdIns(4,5)P_2 in the wing epithelium induce Moe recruitment and phosphorylation in the apical part of the epithelium. Confocal sections of the wing showing the localisation of PH-GFP (**A**,**B**), MoeWT-GFP (**C**,**D**,**I**), MoeTA-GFP (**E**,**F**) and MoeKN-GFP (**G**,**H**) in either wild type (A,C,E,G) or in cells overexpressing the PIP5KI Sktl (B,D,F,H,I,J). GFP-fusion proteins and Sktl were coexpressed in the dorsal half of the disc pouch, using the *apterousGAL4* driver. Sktl overexpression induces the formation of apical membrane protrusions containing high levels of PtdIns(4,5)P_2, as shown by accumulation of the PH-GFP reporter (B, yellow arrowhead). In Sktl-expressing cells, MoeWT-GFP (D) and MoeTA-GFP (F) accumulate in cell apical protrusions (yellow arrowheads). The MoeKN-GFP distribution is not affected by presence of high levels of PtdIns(4,5)P_2 (compare G and H).
(I) Overexpression of Sktl in dorsal cells (marked by MoeWT-GFP, green) triggers accumulation of Moe-*P* (red) in PtdIns(4,5)P_2-rich apical protrusions that belong to the epithelial cells (seen in yellow, white arrowheads) and not the peripodial membrane. The Moe-*P* channel is also shown in grey (I′) and in false colour (I″). Moe-*P* normal levels, as seen in cells not expressing Sktl are labelled with arrows. (**J**) In dorsal Sktl-overexpressing cells Moe-*P* staining (red, white arrowhead) is seen above apical junctions (indicated by Armadillo localisation, green). A small arrow indicates ventral cells not expressing Sktl.
(**K**) Protein extracts from third larval instar imaginal discs corresponding to wild-type flies (control) or flies overexpressing Sktl (UASSktl). Immunoblot with a Moe-*P*-specific antibody (upper panel) shows that overexpression of Sktl increases the fraction of phosphorylated Moe. Equal amounts of Moe protein were loaded in each lane (lower panel). Scale bar: 20 µm A-H; 10 µm I-J.

viability of *Moe* mutant flies, including the strong Moe^{PL54} allele. Detailed examination of wing mosaics containing *Moe* mutant cells further illustrate that phosphorylation of Moe T559 is dispensable for the integrity of this epithelium. These observations indicate that, at least for certain aspects of tissue homeostasis, regulation via PtdIns(4,5)P_2 binding could be sufficient to control Moe distribution and activity, although we cannot formally exclude the possibility that Moe phosphorylation in other unknown residues also contributes to activation of the MoeTA form. Although our results appear in conflict with previous reports (Hipfner et al., 2004; Speck et al., 2003), it is worth noticing that these latter studies used Moe forms carrying a N-terminal Myc tag, which could significantly affect Moe activity. Our results show that Moe proteins tagged with GFP at the C-terminus have a reduced activity when compared with their full-length equivalents. If addition of an N-terminal tag further reduces the activity of tested proteins, it would explain why previous studies failed to detect a rescue with MoeTA (Hipfner et al., 2004; Speck et al., 2003). However, this tag would reduce the toxic effect of MoeTD sufficiently to obtain a weak rescue (Hipfner et al., 2004; Speck et al., 2003), similarly to what we observe expressing an untagged MoeKNTD form.

Our results therefore allow us to postulate the existence of a pool of open, non-phosphorylated Moe molecules that nonetheless can fulfil in vivo their role as linkers between the actin cytoskeleton and the membrane (Fig. 8). The idea that different active ERM forms, phosphorylated and not phosphorylated, could coexist at the cell cortex is also consistent with results from kinetic analyses showing the existence of three different pools of ezrin in the membrane of cultured cells (Coscoy et al., 2002). Although stable and highly mobile molecules could respectively correspond to phosphorylated and PtdIns(4,5)P_2-bound ezrin, the pool of molecules displaying intermediate mobility in the cell cortex could reflect the presence of unphosphorylated ezrin interacting with actin filaments and membrane proteins. In any case, our data provide unambiguous evidence that active ERM protein distribution cannot be faithfully deduced from the ERM phosphorylation pattern.

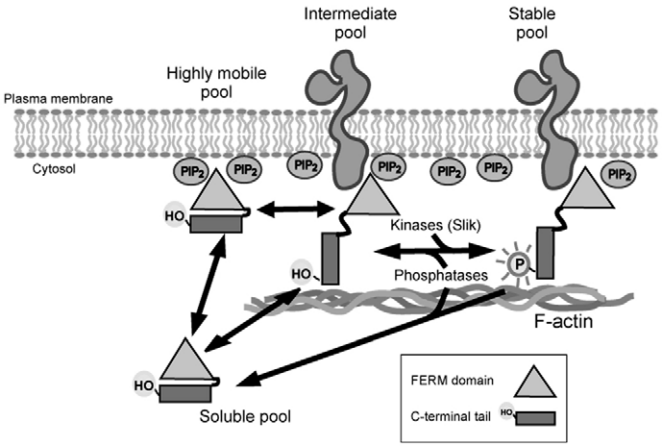

Fig. 8. A general model for the regulation of ERM protein activity. Presence of high levels of PtdIns(4,5)P_2 recruits ERM proteins to the membrane from a cytoplasmic pool of dormant molecules. The non-phosphorylated ERM form can associate with actin filaments and membrane components, such as integral membrane proteins, acting as a link between these two structures. This PtdIns(4,5)P_2-mediated recruitment step is also required for ERM phosphorylation by its specific kinases, such as *Drosophila* Slik. Stable association of ERM proteins with the membrane and the actin cortex, required in specific cellular contexts, is promoted by phosphorylation.

Fine-tuning ERM protein activity

Previous work has shown that Moe has an essential role during eye differentiation, where it is required for the morphogenesis of the highly specialised microvilli that constitute the photoreceptor rhabdomeres (Karagiosis and Ready, 2004). These large membrane protrusions accumulate high levels of PtdIns(4,5)P_2 and phosphorylated Moe (Karagiosis and Ready, 2004; Stauffer et al., 1998; Zelhof and Hardy, 2004). Consistently, our rescue experiments show that eye morphogenesis requires proper Moe regulation by both phosphorylation and PtdIns(4,5)P_2 binding. Although MoeTA is sufficient to restore the viability of *Moe* mutants, the eye phenotype is not suppressed in rescued animals, showing that T559 phosphorylation is crucial in this tissue. Phosphorylation might be essential to provide a stable association between Moe and its partners in these specialised giant villi of the apical domain. The situation in the undifferentiated wing epithelium appears different, because expression of MoeTA in this tissue is enough to ensure epithelial integrity. These results indicate that, depending of the cellular context, transient or stable association of ERM proteins with the cortex can be the preferred choice. Modulation of PtdIns(4,5)P_2 levels would allow a dose-sensitive activation of ERM molecules at the membrane, with phosphorylation being a secondary step necessary for the formation and maintenance of specialised cellular structures.

The aberrant morphology of S2 and wing cells and the developmental lethality induced by MoeTD show that an open form, mimicking a constitutively phosphorylated molecule has strong effects on cell organisation and morphogenesis. Thus, phosphorylation-dephosphorylation cycles are also an important aspect in the regulation of Moe function during development. The ability to cycle between phosphorylated and dephosphorylated Moe has been shown to be necessary for photoreceptor physiology, suggesting that Moe dephosphorylation mediates remodelling of photoreceptor cytoarchitecture in response to light (Chorna-Ornan et al., 2005). Recent work further suggests that local hydrolysis of PtdIns(4,5)P_2 after phospholipase-C (PLC) activation, as it is the case in phototransduction, can contribute to the fast removal of ERM proteins from the plasma membrane (Hao et al., 2009).

A system of double regulation based on activation by PtdIns(4,5)P_2 levels and stabilisation by phosphorylation has evolved to finely tune the activity of ERM proteins in a whole set of different cellular structures and developmental situations. Clearly, this feature contributes to the versatility of ERM proteins and helps to explain why they have a central role in such a varied number of morphogenetic processes.

Materials and Methods

Generation of DMoeKN mutants

Moe cDNA was subcloned in the pGEX-4T1 plasmid, allowing production of GST-Moe fusion protein. MoeKN was generated by mutation of lysine 254, 255, 262, 263 to asparagine, as previously done for human ezrin (Barret et al., 2000). The KN mutations were generated by replacement of the *Nco*I-*Bsp*EI wild-type fragment in pGEX-Moe with a set of overlapping mutant oligonucleotides (Eurogentec). To produce MoeKN GFP-tagged versions, the *Pfl*23II-*Bsp*EI fragment carrying the KN mutation was inserted in the corresponding MoeWT-GFP, MoeTA-GFP, MoeTD-GFP plasmids (Polesello et al., 2002). These constructs were then subcloned into pAc5.1 (Invitrogen) for S2 cell transfection and into pUASp for generation of transgenic lines. For transgenic lines encoding untagged proteins, the full-length *Moe* coding region was amplified by PCR and cloned into pUASp.

Protein expression and purification

Plasmids encoding GST-Moe were used to transform TG1 bacteria. After overnight growth, IPTG (0.5 mM) was added for 1 hour and bacteria centrifuged at 4000 r.p.m. for 15 minutes. All further details refer to 1 litre culture. Bacteria pellets were sonicated in 15 ml PBS containing 5 mM EDTA and protease inhibitors (Complete from Roche). Samples were then centrifuged at 40,000 ***g*** for 30 minutes. Supernatants were diluted to 50 ml and 3 ml glutathione agarose beads slurry (v/v) was added. After incubation for 2 hours at 4°C, beads were washed with 50 mM Tris-HCl, pH 7.4 and 100 mM NaCl. When the OD_{280} was 0, 100 U benzonase was added for 45 minutes at room temperature. After washing the beads, gels were equilibrated in the same buffer supplemented with 2.5 mM $CaCl_2$. Thrombin (50 U) was then added and samples incubated for 1 hour at 37°C. Cleaved proteins were eluted and their concentration calculated, taking into account their extinction coefficient. To avoid interference of calcium with the different assays involving phospholipids, EGTA (5 mM) was added to the recombinant proteins, which were stored at 4°C and used within 48 hours.

Liposome-binding assay

Phospholipids (PC, PS and PE) and PtdIns(4,5)P_2 were purchased from Sigma and Lipid Products (Redhill, UK). Lipids, resuspended in water, were mixed in the appropriate proportions and dried using a Speedvac. Dry pellets were then allowed to swell in 10 mM Tris-HCl, pH 7.4 containing 1 mM EGTA at 42°C for 2 hours. After liposome incubation with the Moe proteins overnight, samples were centrifuged for 30 minutes in a 42.2 Ti rotor (Beckman) at 100,000 ***g***. Supernatant and pellet samples were then analysed by western blotting. Antibodies against Moe and secondary anti-rabbit antibodies coupled to HRP were used at a 1:10,000. Primary antibodies were first incubated with GST-agarose beads to minimize crossreactivity with GST. Blots were developed using the ECL kit (Amersham) and quantification was performed using the ImageJ software.

Cell culture and immunohistochemistry

S2 cells were maintained in Schneider's *Drosophila* medium (GIBCO) supplemented with 10% heat-inactivated FCS (GIBCO) and penicillin-streptomycin. Cells were transfected using Fugene-6 according to the manufacturer's instructions (Roche Diagnostics) and observed 24 hours later. Cells were allowed to spread for 1 hour on No. 1.5 coverslips (Corning) previously treated with 20 µl of 0.5 mg/ml concanavalin A (Sigma) in water and allowed to air dry (Rogers et al., 2002). Cells were then fixed for 20 minutes in BRB80 buffer (80 mM PIPES, pH 6.9, 1 mM $MgCl_2$, 1 mM EGTA) containing 3% formaldehyde (EM Sciences) and 1 mg/ml saponin. Blocking and permeabilisation was performed in TBS (20 mM Tris-HCl, pH 7.5, 154 mM NaCl, 2 mM EGTA, 2 mM $MgCl_2$) containing 2% BSA and 0.02% saponin for 1.5 hours. Coverslips were then incubated for 30 minutes on 20 µl droplets of Texas-Red-phalloidin 1:100 (Molecular Probes) in TBS-BSA-saponin. After washes in TBS-BSA-saponin (15 minutes) and TBS (twice for 15 minutes), coverslips were mounted onto glass slides using Hardset VectaShield (Vector). Images were acquired using a Leica DMIRE2 inverted microscope with a MICROMAX-1300Y-HS cooled camera (Princeton Instrument). Fluorescence levels were quantified by analysing image stacks (recorded using the same settings) with the ImageJ software (http://rsbweb.nih.gov/ij). Morphometry analyses were performed using calculation of the circularity index of ImageJ.

Wing discs were dissected in PBS, fixed for 20 minutes in paraformaldehyde 4% in PBS and incubated overnight in Rhodamine phalloidin (Sigma) and 10 mM Topro3

(Molecular Probes) in PBS-Tween 0.1%. After three 30 minutes washes in PBS 0.1% Tween20, discs were mounted in Vectashield (Vector). Primary antibodies were rabbit anti-Moe-*P*, 1:500 (Karagiosis and Ready, 2004), rabbit anti-activated Caspase3, 1:100 (Cell Signalling), mouse anti-arm, 1:100 (DSHB). We used as secondary antibodies Rhodamine anti-rabbit, FITC anti-mouse and Cy5 anti-mouse, all diluted 1:300 (Jackson Laboratories). For immunostaining, discs were fixed as above and incubated overnight with the corresponding primary antibody dilutions in PBS 0.3% Triton X-100, 1% BSA. Samples were visualised with a Leica TCS SP2 confocal microscope. False colours images were generated applying the Rainbow LUT of the ImageJ software to disc pictures obtained using the same confocal settings.

Fly strains

The following strains were used: *ywMoe*^{PL54}, *ywMoe*^{PL106} (Polesello et al., 2002), *ywFRT19A*, *tubulin-GAL4*^{LL7} (Lee and Luo, 1999), *apterousGAL4*^{md544} (Calleja et al., 1996), *UASMoeWT-GFP*, *UASMoeTA-GFP*, *UASMoeTD-GFP* (Polesello et al., 2002), *UASPH-GFP* (Zelhof and Hardy, 2004), *sktl*$^{\Delta 5}$ and *UASSktl* (Hassan et al., 1998) and *UASp35*^{BH2} (Hay et al., 1994). The transgenic lines *UASMoeWT*, *UASMoeKN*, *UASMoeTA*, *UASMoeTD*, *UASMoeKNTA*, *UASMoeKNTD*, *UASMoeKN-GFP*, *UASMoeKNTA-GFP* and *UASMoeKNTD-GFP* were generated in this work. For rescue experiments, *ywMoe*^{PL54}*/FM6; tubulin-GAL4*^{LL7}*/TM2* and *ywMoe*^{PL106}*/FM6; tubulin-GAL4*^{LL7}*/TM2* females were crossed to males carrying the different *UASMoe*^{Mut} insertions in an autosome. We calculated for each cross the ratio between the observed number of *ywMoe*$^{-}$*; tubulin-GAL4LL7/UASMoe*^{Mut} surviving males and the *ywMoe*$^{-}$*/+; TM2/UASMoe*^{Mut} female siblings. This ratio should be 1 for a total rescue. Wing disc clones were generated using the MARCM system (Lee and Luo, 1999), giving 1 hour heatshock at 37°C to first instar larvae. *Moe*$^{PL106/PL106}$ positively labelled cells were generated in *ywMoe*^{PL106} *FRT19A/hsFLP*^{1} *tubulin-GAL80*^{LL1} *FRT19A; UASmCD8GFP*^{LL5}*/+; tubulin-GAL4*^{LL7}*/+* females. The *Moe*$^{PL106/PL106}$ mutant clones rescued by the different Moe^{Mut}-GFP versions were obtained using the stocks *ywMoe*^{PL106} *FRT19A/ hsFLP*^{1} *tubulin-GAL80*^{LL1} *FRT19A; UASMoe*^{Mut}*-GFP/+; tubulin-GAL4*^{LL7}*/+*. The *sktl*$^{\Delta 5}$ mutant clones were observed in larvae of the genotype *elav*^{C155} *UASmCD8GFP*^{LL4} *hsFLP*^{1}; *FRTG13 tubulin-GAL80*^{LL2}*/FRTG13 sktl*^{D5}; *tubulin-GAL4*^{LL7}*/UASp35* ^{BH2}. All crosses were done at 25°C.

Cuticle imaging

Adult flies were dehydrated in absolute ethanol, coated with colloidal gold and visualised with a Hitachi scanning electron microscope. Wings were mounted in 6:5 ethanol:lactic acid and visualised with a Zeiss Axiophot microscope.

Analysis of fly extracts

30 wing imaginal discs per genotype were dissected in PBS, pooled together, brought to 20 µl with PBS and homogenised by boiling in 10 µl of 3× Laemmli buffer. Then, 20 µl homogenate was loaded on an SDS-PAGE gel for immunodetection with anti-Moe-*P* antibody. 3 µl of the same sample was loaded on a different gel for immunodetection with anti-Moe used at 1:50,000. Four adult flies for each genotype were homogenised in 100 µl of boiling Laemmli 3× buffer and 5 µl homogenate was loaded on an SDS-PAGE gel and blotted with anti-Moe or anti-Moe-*P* in the same conditions. Signal was detected using the ECL kit from Amersham.

We are grateful to H. Bellen, D. Ready, A. Zelhof, the Bloomington Stock Center and the Iowa DSHB for stocks and antibodies. We also wish to thank three anonymous referees for their constructive comments on the manuscript. This work was supported by grants from the ACI Biologie du Développement et Physiologie Intégrative (030023), ARC (3832), FRM (Equipe 2005) and the Canadian Institutes for Health Research (MOP-89877). C.P. was supported by the Ministère de la Recherche and ARC (1114), C.R. by the Ministère de la Recherche and a Lavoisier fellowship. S.C. is a FRSQ 'Junior I' fellow. F.R. benefited from a Long Term EMBO fellowship.

Supplementary material available online at
http://jcs.biologists.org/cgi/content/full/123/12/2058/DC1

References

Barret, C., Roy, C., Montcourrier, P., Mangeat, P. and Niggli, V. (2000). Mutagenesis of the phosphatidylinositol 4,5-bisphosphate (PIP(2)) binding site in the NH(2)-terminal domain of ezrin correlates with its altered cellular distribution. *J. Cell Biol.* **151**, 1067-1080.

Brand, A. H. and Perrimon, N. (1993). Targeted gene expression as a means of altering cell fates and generating dominant phenotypes. *Development* **118**, 401-415.

Bretscher, A., Edwards, K. and Fehon, R. G. (2002). ERM proteins and merlin: integrators at the cell cortex. *Nat. Rev. Mol. Cell Biol.* **3**, 586-599.

Calleja, M., Moreno, E., Pelaz, S. and Morata, G. (1996). Visualization of gene expression in living adult Drosophila. *Science* **274**, 252-255.

Carreno, S., Kouranti, I., Glusman, E. S., Fuller, M. T., Echard, A. and Payre, F. (2008). Moesin and its activating kinase Slik are required for cortical stability and microtubule organization in mitotic cells. *J. Cell Biol.* **180**, 739-746.

Chorna-Ornan, I., Tzarfaty, V., Ankri-Eliahoo, G., Joel-Almagor, T., Meyer, N. E., Huber, A., Payre, F. and Minke, B. (2005). Light-regulated interaction of Dmoesin with TRP and TRPL channels is required for maintenance of photoreceptors. *J. Cell Biol.* **171**, 143-152.

Coscoy, S., Waharte, F., Gautreau, A., Martin, M., Louvard, D., Mangeat, P., Arpin, M. and Amblard, F. (2002). Molecular analysis of microscopic ezrin dynamics by two-photon FRAP. *Proc. Natl. Acad. Sci. USA* **99**, 12813-12818.

Fievet, B. T., Gautreau, A., Roy, C., Del Maestro, L., Mangeat, P., Louvard, D. and Arpin, M. (2004). Phosphoinositide binding and phosphorylation act sequentially in the activation mechanism of ezrin. *J. Cell Biol.* **164**, 653-659.

Gary, R. and Bretscher, A. (1995). Ezrin self-association involves binding of an N-terminal domain to a normally masked C-terminal domain that includes the F-actin binding site. *Mol. Biol. Cell* **6**, 1061-1075.

Gervais, L., Claret, S., Januschke, J., Roth, S. and Guichet, A. (2008). PIP5K-dependent production of PIP2 sustains microtubule organization to establish polarized transport in the Drosophila oocyte. *Development* **135**, 3829-3838.

Hamada, K., Shimizu, T., Matsui, T., Tsukita, S. and Hakoshima, T. (2000). Structural basis of the membrane-targeting and unmasking mechanisms of the radixin FERM domain. *EMBO J.* **19**, 4449-4462.

Hao, J. J., Liu, Y., Kruhlak, M., Debell, K. E., Rellahan, B. L. and Shaw, S. (2009). Phospholipase C-mediated hydrolysis of PIP2 releases ERM proteins from lymphocyte membrane. *J. Cell Biol.* **184**, 451-462.

Hassan, B. A., Prokopenko, S. N., Breuer, S., Zhang, B., Paululat, A. and Bellen, H. J. (1998). skittles, a Drosophila phosphatidylinositol 4-phosphate 5-kinase, is required for cell viability, germline development and bristle morphology, but not for neurotransmitter release. *Genetics* **150**, 1527-1537.

Hay, B. A., Wolff, T. and Rubin, G. M. (1994). Expression of baculovirus P35 prevents cell death in Drosophila. *Development* **120**, 2121-2129.

Hayashi, K., Yonemura, S., Matsui, T. and Tsukita, S. (1999). Immunofluorescence detection of ezrin/radixin/moesin (ERM) proteins with their carboxyl-terminal threonine phosphorylated in cultured cells and tissues. *J. Cell Sci.* **112**, 1149-1158.

Hipfner, D. R., Keller, N. and Cohen, S. M. (2004). Slik Sterile-20 kinase regulates Moesin activity to promote epithelial integrity during tissue growth. *Genes Dev.* **18**, 2243-2248.

Karagiosis, S. A. and Ready, D. F. (2004). Moesin contributes an essential structural role in Drosophila photoreceptor morphogenesis. *Development* **131**, 725-732.

Khanna, C., Wan, X., Bose, S., Cassaday, R., Olomu, O., Mendoza, A., Yeung, C., Gorlick, R., Hewitt, S. M. and Helman, L. J. (2004). The membrane-cytoskeleton linker ezrin is necessary for osteosarcoma metastasis. *Nat. Med.* **10**, 182-186.

Kunda, P., Pelling, A. E., Liu, T. and Baum, B. (2008). Moesin controls cortical rigidity, cell rounding, and spindle morphogenesis during mitosis. *Curr. Biol.* **18**, 91-101.

Lee, T. and Luo, L. (1999). Mosaic analysis with a repressible cell marker for studies of gene function in neuronal morphogenesis. *Neuron* **22**, 451-461.

Matsui, T., Maeda, M., Doi, Y., Yonemura, S., Amano, M., Kaibuchi, K. and Tsukita, S. (1998). Rho-kinase phosphorylates COOH-terminal threonines of ezrin/radixin/moesin (ERM) proteins and regulates their head-to-tail association. *J. Cell Biol.* **140**, 647-657.

McCartney, B. M. and Fehon, R. G. (1996). Distinct cellular and subcellular patterns of expression imply distinct functions for the Drosophila homologues of moesin and the neurofibromatosis 2 tumor suppressor, merlin. *J. Cell Biol.* **133**, 843-852.

Nakamura, F., Huang, L., Pestonjamasp, K., Luna, E. J. and Furthmayr, H. (1999). Regulation of F-actin binding to platelet moesin in vitro by both phosphorylation of threonine 558 and polyphosphatidylinositides. *Mol. Biol. Cell* **10**, 2669-2685.

Niggli, V., Andreoli, C., Roy, C. and Mangeat, P. (1995). Identification of a phosphatidylinositol-4,5-bisphosphate-binding domain in the N-terminal region of ezrin. *FEBS Lett.* **376**, 172-176.

Pearson, M. A., Reczek, D., Bretscher, A. and Karplus, P. A. (2000). Structure of the ERM protein moesin reveals the FERM domain fold masked by an extended actin binding tail domain. *Cell* **101**, 259-270.

Polesello, C. and Payre, F. (2004). Small is beautiful: what flies tell us about ERM protein function in development. *Trends Cell. Biol.* **14**, 294-302.

Polesello, C., Delon, I., Valenti, P., Ferrer, P. and Payre, F. (2002). Dmoesin controls actin-based cell shape and polarity during Drosophila melanogaster oogenesis. *Nat. Cell Biol.* **4**, 782-789.

Rasmussen, M., Alexander, R. T., Darborg, B. V., Mobjerg, N., Hoffmann, E. K., Kapus, A. and Pedersen, S. F. (2008). Osmotic cell shrinkage activates ezrin/radixin/moesin (ERM) proteins: activation mechanisms and physiological implications. *Am. J. Physiol. Cell Physiol.* **294**, C197-C212.

Rogers S. L, Rogers G. C, Sharp D. J, Vale R. D. (2002). Drosophila EB1 is important for proper assembly, dynamics, and positioning of the mitotic spindle. *J. Cell Biol.***158**, 873-884.

Speck, O., Hughes, S. C., Noren, N. K., Kulikauskas, R. M. and Fehon, R. G. (2003). Moesin functions antagonistically to the Rho pathway to maintain epithelial integrity. *Nature* **421**, 83-87.

Stauffer, T. P., Ahn, S. and Meyer, T. (1998). Receptor-induced transient reduction in plasma membrane PtdIns(4,5)P2 concentration monitored in living cells. *Curr. Biol.* **8**, 343-346.

Turunen, O., Wahlstrom, T. and Vaheri, A. (1994). Ezrin has a COOH-terminal actin-binding site that is conserved in the ezrin protein family. *J. Cell Biol.* **126**, 1445-1453.

Yin, H. L. and Janmey, P. A. (2003). Phosphoinositide regulation of the actin cytoskeleton. *Annu. Rev. Physiol.* **65**, 761-789.

Yonemura, S., Matsui, T. and Tsukita, S. (2002). Rho-dependent and -independent activation mechanisms of ezrin/radixin/moesin proteins: an essential role for polyphosphoinositides in vivo. *J. Cell Sci.* **115**, 2569-2580.

Yu, Y., Khan, J., Khanna, C., Helman, L., Meltzer, P. S. and Merlino, G. (2004). Expression profiling identifies the cytoskeletal organizer ezrin and the developmental homeoprotein Six-1 as key metastatic regulators. *Nat. Med.* **10**, 175-181.

Zelhof, A. C. and Hardy, R. W. (2004). WASp is required for the correct temporal morphogenesis of rhabdomere microvilli. *J. Cell Biol.* **164**, 417-426.